

FL

12



AD A 024285

MICROSTRUCTURE ANALYSIS
FINAL REPORT
VOLUME I
THE ORIGIN OF OCEAN FINE STRUCTURE

SEPTEMBER 30, 1975

by
GIRARD A. SIMONS

Sponsored by
Advanced Research Projects Agency
ARPA Order No. 2961

Contract No. N00014-75-C-0927

DDC
RECORDED
MAY 11 1976
B

PHYSICAL SCIENCES INC.
18 LAKESIDE OFFICE PARK, WAKEFIELD, MASSACHUSETTS

UNLIMITED DISTRIBUTION

The views and conclusions contained in this document are those of the authors and should not be interpreted as necessarily representing the official policies, either expressed or implied, of the Advanced Research Projects Agency or the U. S. Government.

ACCESSION for	
NTIS	White Section <input checked="" type="checkbox"/>
DOC	Gov. Section <input type="checkbox"/>
UNCLASSIFIED	<input type="checkbox"/>
JUSTIFICATION	
BY	
DISTRIBUTION AVAILABILITY CODES	
Dist.	MAIL. Ctr./OF SERIAL

[Handwritten signature and scribbles over the form]

UNCLASSIFIED

SECURITY CLASSIFICATION OF THIS PAGE (When Data Entered)

REPORT DOCUMENTATION PAGE		READ INSTRUCTIONS BEFORE COMPLETING FORM
1. REPORT NUMBER	2. GOVT ACCESSION NO.	3. RECIPIENT'S CATALOG NUMBER
4. TITLE (and Subtitle) MICROSTRUCTURE ANALYSIS. Volume I. The Origin of Ocean Fine Structure.		5. TYPE OF REPORT & PERIOD COVERED Final Report 2/15/75 - 8/15/75
7. AUTHOR(s) Girard A. Simons		6. PERFORMING ORG. REPORT NUMBER PSI-TR-36
9. PERFORMING ORGANIZATION NAME AND ADDRESS Physical Sciences Inc. 18 Lakeside Office Park Wakefield, MA 01880		8. CONTRACT OR GRANT NUMBER(s) N00014-75-C-0927
11. CONTROLLING OFFICE NAME AND ADDRESS Office of Naval Research Department of the Navy Arlington, VA 22217		10. PROGRAM ELEMENT, PROJECT, TASK AREA & WORK UNIT NUMBERS WARPA Order No. 2961
14. MONITORING AGENCY NAME & ADDRESS (if different from Controlling Office) 12) 49 p.		12. REPORT DATE Sept 30 1975
		13. NUMBER OF PAGES 44
		15. SECURITY CLASS. (of this report) Unclassified
		15a. DECLASSIFICATION/DOWNGRADING SCHEDULE
16. DISTRIBUTION STATEMENT (of this Report) Unlimited distribution		
17. DISTRIBUTION STATEMENT (of the abstract entered in Block 20, if different from Report) Final rept. 15 Feb - 15 Aug 75,		
18. SUPPLEMENTARY NOTES		
19. KEY WORDS (Continue on reverse side if necessary and identify by block number) Internal Waves Inertial Waves Ocean Fine Structure Ocean Microstructure		
20. ABSTRACT (Continue on reverse side if necessary and identify by block number) The horizontal and vertical length scales of ocean fine structure appear to correlate to the corresponding wavelengths of inertial waves (internal waves whose motion is dominated by Coriolis forces). A priori, there are four possible non-linear mechanisms that could form ocean fine structure from inertial waves: dynamic breaking (shear instabilities), static breaking (inverted density profile), trans - (cont on p 1473 B)		

391 105

UNCLASSIFIED

SECURITY CLASSIFICATION OF THIS PAGE(When Data Entered)

(cont fr p 1473A)
verse steepening (resonance) and longitudinal steepening (self steepening of waves riding on their own velocity fields). Each mechanism has been assessed, on the basis of the available data. Of the four mechanisms proposed, dynamic wave breaking ^{is} shown to be the most probable mechanism by which inertial waves form fine structure. This mechanism is distinct from that of "billow turbulence" due to an unstable, horizontally propagating gravity wave. An inertial wave is a vertically propagating transverse wave. The transverse velocity field of the wave is a horizontal shear layer and it is the instability of the shear layer that is the proposed source of fine structure.

A

(1473B)

UNCLASSIFIED

SECURITY CLASSIFICATION OF THIS PAGE(When Data Entered)

MICROSTRUCTURE ANALYSIS
FINAL REPORT
VOLUME I
THE ORIGIN OF OCEAN FINE STRUCTURE

SEPTEMBER 30, 1975

ARPA Order Number 2961
Program Code No. 5E10
Name of Contractor: Physical Sciences Inc.
18 Lakeside Office Park
Wakefield, Mass. 01880
Effective Date of Contract: February 15, 1975
Contract Expiration Date: August 15, 1975
Amount of Contract: \$51,081.00
Contract Number: N00014-75-C-0927
Principal Investigator: Girard A. Simons
Telephone Number: (617) 245-7400
Scientific Officer: Office of Naval Research, Code 212
800 North Quincy Street
Arlington, Virginia 22217
Attn: Cdr. Donald D. Pizinger
Title: Microstructure Analysis

ACCESSION NO.	
NTS	DATE FORW. <input checked="" type="checkbox"/>
DTG	DATE FORW. <input type="checkbox"/>
DTG	DATE FORW. <input type="checkbox"/>
BY	
DATE	
A	

Sponsored by
Advanced Research Projects Agency
ARPA Order No. 2961

FOREWORD

Volume I of the Final Report deals with Ocean Micro-structure and Volume II deals with Laser Sensor Technology Assessment.

ABSTRACT

The horizontal and vertical length scales of ocean fine structure appear to correlate to the corresponding wavelengths of inertial waves (internal waves whose motion is dominated by Coriolis forces). A priori, there are four possible non-linear mechanisms that could form ocean fine structure from inertial waves: dynamic breaking (shear instabilities), static breaking (inverted density profile), transverse steepening (resonance) and longitudinal steepening (self steepening of waves riding on their own velocity fields). Each mechanism has been assessed on the basis of the available data. Of the four mechanisms proposed, dynamic wave breaking is shown to be the most probable mechanism by which inertial waves form fine structure. This mechanism is distinct from that of "billow turbulence" due to an unstable, horizontally propagating gravity wave. An inertial wave is a vertically propagating transverse wave. The transverse velocity field of the wave is a horizontal shear layer and it is the instability of the shear layer that is the proposed source of fine structure.

TABLE OF CONTENTS

	<u>Page</u>
ABSTRACT	iii
I. INTRODUCTION	1
II. INTERNAL WAVE SOLUTIONS	7
III. COMPARISON OF FINE STRUCTURE DATA WITH INTERNAL WAVES	15
IV. CONCLUSIONS	27
REFERENCES	31
APPENDIX A	A-1

LIST OF ILLUSTRATIONS

		<u>Page</u>
Fig. 1	Idealized Ocean Fine Structure	3
Fig. 2	Temperature Gradient Record Reproduced from Gregg Cox and Hacker. ⁶ The plot begins at 215 m in the upper left hand corner and ends at 400 m at the lower right. The total length of the arrow represents 10 m in depth, Z positive upward.	4
Fig. 3	Coordinate System on Rotating Earth	8
Fig. 4	Density Profile Corresponding to a Statically Stable Internal Wave	13
Fig. 5	Density Profile Corresponding to a Statically Unstable Internal Wave	14
Fig. 6	Comparison of Internal Waves with Fine Structure	16
Fig. 7	Wave Amplitude Required for Instability	19
Fig. 8	Inertial Wave Stability	22
Fig. 9	Estimates of Self Steepening Times	25
Fig. 10a	Woods Postulate of Billow Turbulence	29
Fig. 10b	Proposed Source of Ocean Fine Structure	29
Fig. A-1	Internal Wave Regimes	A-10

I. INTRODUCTION

Field observations¹⁻⁸ have revealed that the ocean's density profile possesses an internal structure consisting of a series of thin, laminar "sheets" of high density gradient separated by "steps" of only moderate gradient. An idealized "fine structure" is represented schematically in Fig. 1. Only Woods' observation¹ reveals the more distinct step-like structure. Later observations²⁻⁸ illustrate more irregular profiles with a fine structure of height H and a superimposed microstructure on a length scale small with respect to H . One of the more irregular profiles is illustrated in Fig. 2 which is reproduced from Gregg, Cox and Hacker.⁶ The recording demonstrates temperature gradient as a function of depth. The "spikes" in the temperature gradient correspond to the "sheets" of high gradient and the small scale structure in the temperature gradient represents the microstructure which is actually present in the "steps" of the idealized fine structure.

The "step height" H and the lateral extent of the observed structure varies widely over the range of mean density gradient indicated in Table I. The observation time refers to the time spent taking soundings at various lateral locations whereas the point persistence time refers to the time duration between soundings at a given lateral location. The term persistence need not necessarily imply that the same structure remained for the duration of the persistence time. It is always possible that a second similar structure occupied the same point at a later time.

Various mechanisms have been proposed to explain the observed phenomenon. These mechanisms consist of double diffusion,⁹ interleaving,¹⁰ dynamic breaking of internal gravity waves¹¹ due to shear instabilities and the static breaking of internal waves¹² due to the associated density inversions.

This paper is not intended to be a review or assessment of the proposed mechanisms. What we wish to do is to investigate the possibility that internal waves are responsible for the generation of fine structure. Due to the sparse amount of data available, we can only attempt to determine a mechanism which is at least not inconsistent with data. Hereafter, the terms consistent and apparent correlation shall be used to infer that the data does not demonstrate otherwise.

The internal wave solutions are briefly reviewed in Sec. II. To avoid ambiguities, let us adopt the notation that inertial waves are internal waves in which the Coriolis forces play a dominant role. Inertial waves propagate "almost" vertically with a frequency related to the earth's rotational frequency. On the other hand, gravity waves are internal waves which are dominated by buoyancy while Coriolis forces play a secondary role. In Sec. III, the length scales of internal waves are compared to those of the fine structure and it appears that only inertial waves can be responsible for fine structure. This suggests that a mechanism by which inertial waves could form fine structure is inherent in the difference between inertial waves and gravity waves. One such mechanism is shown to be the shear instability of the wave. Inertial waves are much less stable to the Kelvin Helmholtz instability than are gravity waves. Other mechanisms are suggested which could transform the inertial wave into fine structure but they are shown to be considerably less probable than dynamic breaking. This strongly indicates that shear instabilities are the mechanism by which inertial waves form fine structure. Previous investigators¹¹ have proposed that shear instabilities lead to ocean fine structure. However, their concept of "billow turbulence" due to a horizontally propagating gravity wave is quite different from the present concept of an unstable, vertically propagating inertial wave. A physical description of the proposed model and its distinction from "billow turbulence" is given in the Conclusions.

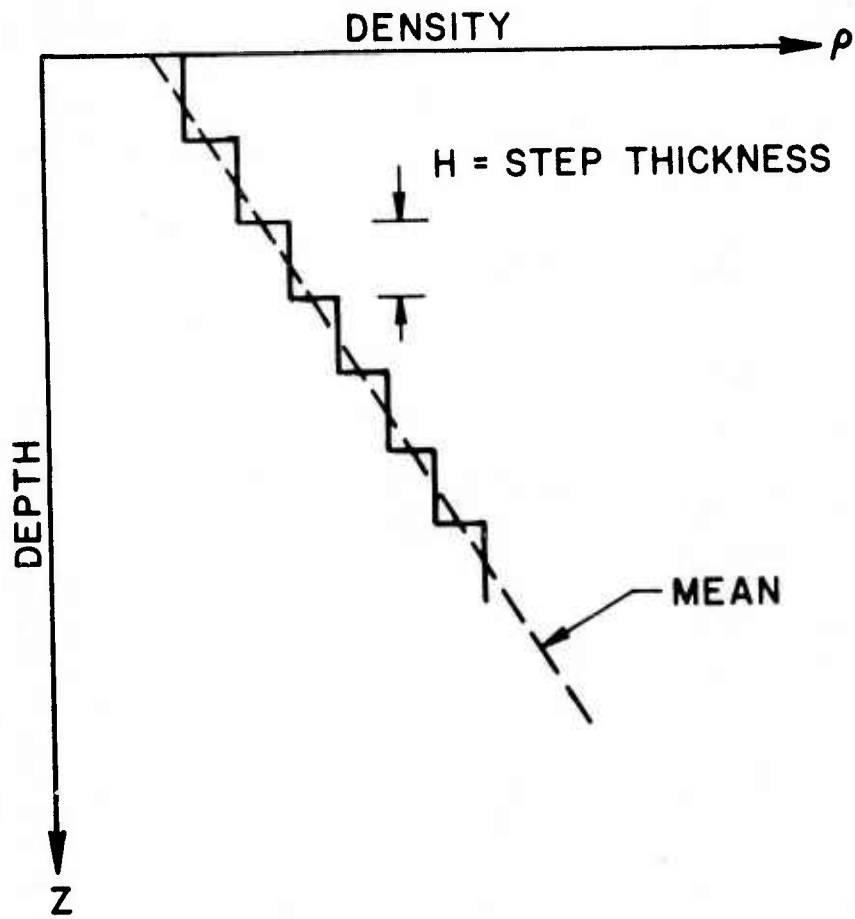


Fig. 1 Idealized Ocean Fine Structure

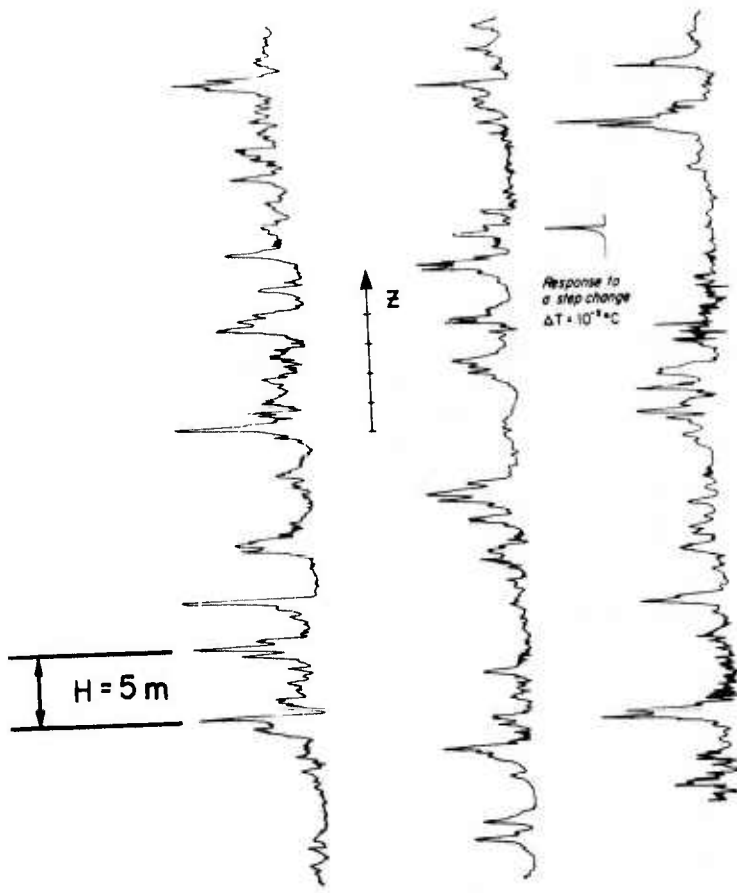


Fig. 2 Temperature Gradient Record Reproduced from Gregg Cox and Hacker.⁶ The plot begins at 215 m in the upper left hand corner and ends at 400 m at the lower right. The total length of the arrow represents 10 m in depth, Z positive upward.

TABLE I

FINE STRUCTURE DATA BASE

<u>Observer</u>	<u>Grad ($\frac{\Delta\rho}{\rho}$)</u>	<u>H</u>	<u>Lateral Extent</u>	<u>Observation Time</u>	<u>Point Persistence Time</u>
Woods (1)	O (10^{-4} /m)	O (1-2 m)	?	?	?
Howe & Tait (2)	O (10^{-6} /m)	O (35 m)	O (10 miles)	3 days	> 33 hrs.
Simpson (3)	O (10^{-5} /m)	O (10-20 m)	O (1-3 km)	3 days	?
Gregg & Cox (4)	O (3×10^{-6} /m)	O (5 m)	O (1-5 km)*	1 hour	?
Gregg et al. (6)	O (4×10^{-6} /m)	O (5 m)	O (~2 km)**	14 days	?
Hayes et al. (7)	O (3×10^{-6} /m)	O (10 m)	?	3 days	> 3 days

* Gregg & Cox (4) do not report the lateral dimension. Existing data from Osborn and Cox (5) and Gregg (8) for measurements in the same location (San Diego Through).

** M. C. Gregg, private communication.

II. INTERNAL WAVE SOLUTIONS

The mathematical description of internal waves is a classic oceanographic problem. For wave frequencies near the earth's rotational frequency, the Coriolis forces must be included. Phillips⁽¹³⁾ gives an account of the wave solutions in the presence of Coriolis forces but that solution is carried only as far as obtaining the wave dispersion equation. The wave solutions for the velocity and density are necessary in order to relate ocean fine structure to internal waves. Hence, we must expand on Phillip's results. The details are given in Appendix A and only the highlights of the model and solutions are discussed here.

We adopt a locally orthogonal system on the surface of a rotating earth. The earth's rotational frequency is $\tilde{\Omega}/2$ and the coordinate system is illustrated in Fig. 3. The momentum equations include buoyancy, viscosity, and the Coriolis forces. The flow is assumed to be incompressible, that is, the convective derivative of density is zero. The incompressible continuity equation is used to close the set of equations in pressure, density and velocity. To obtain a solution to the dynamic equations, we assume that the only velocities are those due to the internal waves and we shall expand the density and pressure into a static and wave contribution:

$$\tilde{\rho} = \tilde{\rho}_o + \tilde{\rho}_s(\tilde{z}) + \tilde{\rho}_w(\tilde{x}, \tilde{y}, \tilde{z}, \tilde{t}), \quad (1)$$

and

$$\tilde{p} = \tilde{p}_o - \tilde{\rho}_o \tilde{g} \tilde{z} + \tilde{p}_s(\tilde{z}) + \tilde{p}_w(\tilde{x}, \tilde{y}, \tilde{z}, \tilde{t}), \quad (2)$$

where the superscript \sim denotes a dimensional quantity.

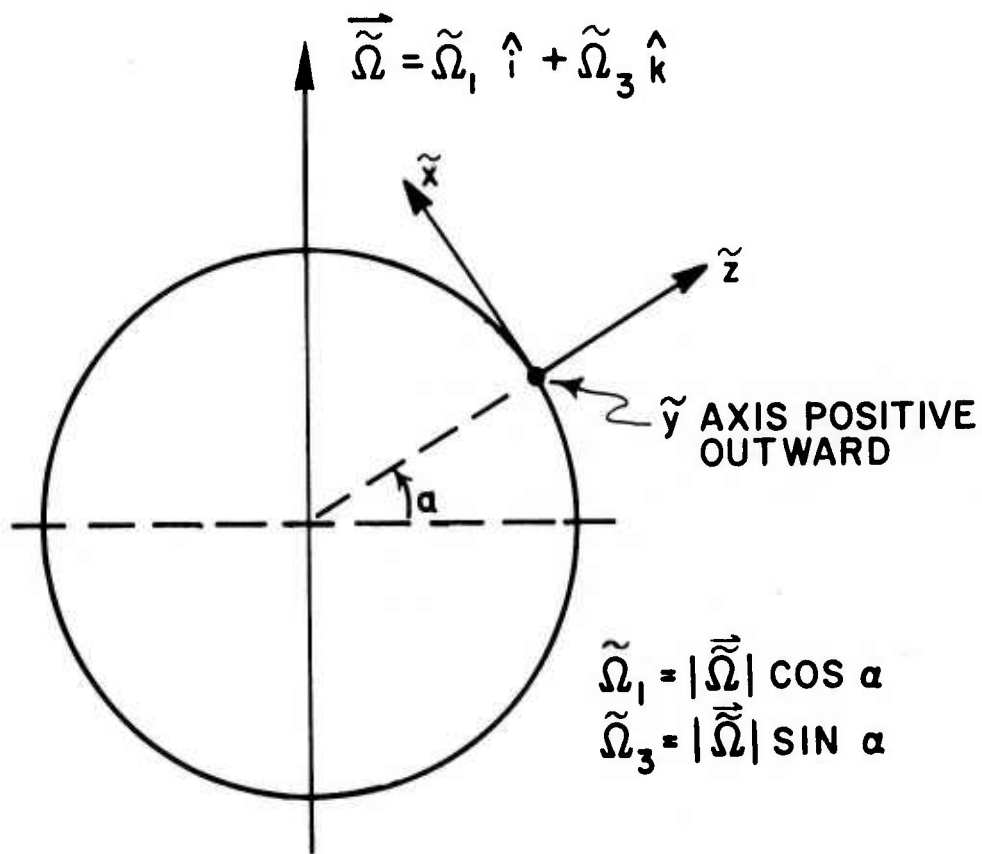


Fig. 3 Coordinate System on Rotating Earth

The static density gradient must be specified "a priori". Hence we assert that

$$\frac{\partial \tilde{\rho}_s}{\partial \tilde{z}} = -\tilde{\beta} \tilde{\rho}_o, \quad (3)$$

where $\tilde{\rho}_o$ is the reference density at $\tilde{z} = 0$. The value of $\tilde{\beta}$ is expressed in units of inverse length and has values between $10^{-4}/\text{m}$ in the summer thermocline and $10^{-6}/\text{m}$ in the deep sea. The density gradient is related to the Brunt Väisälä frequency, \tilde{N} , by

$$\tilde{N} = (\tilde{g} \tilde{\beta})^{1/2}, \quad (4)$$

where \tilde{g} is the acceleration of gravity.

In developing internal wave solutions, we introduce the following dimensional variables: $\tilde{\sigma}$, the wave frequency; \tilde{k}_H , the horizontal wave number; \tilde{k}_V , the vertical wave number and \tilde{u}_p , the fluid velocity in the horizontal direction. These dimensional quantities are used to define four dimensionless parameters:

$$\epsilon = \tilde{u}_p \tilde{k}_H / \tilde{\sigma} \quad (\text{Wave Amplitude}),$$

$$\Lambda = \tilde{\beta} / \tilde{k}_V \quad (\text{Static } \Delta\rho/\rho \text{ Across Wave}),$$

$$\delta_V = \tilde{k}_H / \tilde{k}_V \quad (\text{Vertical/Horizontal Length Scale}),$$

and

$$\text{Re}_w = \tilde{\rho}_o \tilde{\sigma} / \mu \tilde{k}_V^2 \quad (\text{Wave Reynolds Number}).$$

Under the assumptions that \tilde{N} is a constant, $\epsilon \ll 1$ (linearization), $\Lambda \ll 1$ (Boussinesq approximation) and $\text{Re}_w \gg 1$ (Inviscid), the dispersion equation becomes

$$\tilde{\sigma}^2 = \tilde{N}^2 \delta_v^2 / (1 + \delta_v^2) + (\tilde{\Omega} \cdot \hat{\mu})^2, \quad (5)$$

where $\hat{\mu}$ is a unit vector in the direction of wave propagation. For $\delta_v \ll 1$, $\hat{\mu}$ becomes

$$\hat{\mu} = \hat{k} + O(\delta_v \hat{i}) + O(\delta_v \hat{j}).$$

Clearly, for $\delta_v \ll 1$, the internal waves propagate almost vertically.

The connection between ocean fine structure and this type of internal wave is yet to be established but the discussion will be restricted to this limit.

The simplified dispersion equation becomes, for $\delta_v \ll 1$,

$$\tilde{\sigma}^2 = \tilde{N}^2 \delta_v^2 + \tilde{\Omega}_3^2, \quad (6)$$

where $\tilde{\Omega}_3 = \tilde{\Omega} \sin \alpha$, $\tilde{\Omega} = 2\pi$ radians/12 hours and α is the latitude.

The wave solution for the density is

$$\tilde{\rho}_w = (\tilde{\rho}_0 \epsilon \tilde{\theta}/\tilde{k}_v) \exp(i \tilde{\zeta}), \quad (7)$$

and the wave function $\tilde{\zeta}$ is given by

$$\tilde{\zeta} = \tilde{\sigma} \tilde{t} + \tilde{k}_x \tilde{x} + \tilde{k}_y \tilde{y} + \tilde{k}_v \tilde{z},$$

where \tilde{k}_x and \tilde{k}_y are the wave numbers in the \tilde{x} and \tilde{y} directions respectively.

In order to obtain solutions for the fluid velocity in the \tilde{x} and \tilde{y} directions, we utilize the limits suggested by Eq. (6). The frequency $\tilde{\sigma}$ consists of a contribution due to gravity, $\tilde{N}^2 \delta_v^2$, and an inertial contribution, $\tilde{\Omega}_3^2$. The dominance of the buoyant term gives rise to gravity waves whereas the dominance of the Coriolis forces leads to inertial waves.

For Gravity Waves ($\tilde{N} \delta_v > \tilde{\Omega}_3$), the solutions become

$$\tilde{\sigma} = \tilde{N} \delta_v, \quad (8)$$

$$\tilde{u}_w = -i (\tilde{k}_x / \tilde{k}_H) \tilde{u}_p \exp(i \tilde{\xi}), \quad (9)$$

and

$$\tilde{v}_w = -i (\tilde{k}_y / \tilde{k}_H) \tilde{u}_p \exp(i \tilde{\xi}), \quad (10)$$

where

$$\tilde{k}_x^2 + \tilde{k}_y^2 = \tilde{k}_H^2.$$

For Inertial Waves ($\tilde{\Omega}_3 > \tilde{N} \delta_v$), we obtain

$$\tilde{\sigma} = \tilde{\Omega}_3, \quad (11)$$

$$\tilde{u}_w = -\tilde{u}_p (\tilde{k}_y / \tilde{k}_H + i \tilde{k}_x / \tilde{k}_H) \exp(i \tilde{\xi}), \quad (12)$$

and

$$\tilde{v}_w = -i \tilde{u}_p (\tilde{k}_y / \tilde{k}_H + i \tilde{k}_x / \tilde{k}_H) \exp(i \tilde{\xi}). \quad (13)$$

An arbitrary sum of the plane wave solutions over all positive and negative wave numbers is a solution to the equations of motion if and only if ϵ is much less than unity. However, due to the transverse nature of the waves, situations do exist where the nonlinear terms are identically zero and the solutions are valid for arbitrary ϵ . Two such solutions correspond to the single plane wave and the Resonant Triad.⁽¹⁴⁾ Using one plane wave and choosing the time and horizontal location such that the wave amplitude is a maximum, we express the total density profile for arbitrary ϵ ,

$$\frac{(\tilde{\rho} - \tilde{\rho}_o)}{\tilde{\beta} \tilde{\lambda}_v \tilde{\rho}_o} = -\tilde{z}/\tilde{\lambda}_v + \left(\frac{\epsilon}{2\pi}\right) \sin\left(\frac{2\pi\tilde{z}}{\tilde{\lambda}_v}\right), \quad (14)$$

where $\tilde{\lambda}_v$ is $2\pi/\tilde{k}_v$. Eq. (14) is illustrated in Fig. 4 for $\epsilon = 1$. The density profile illustrates an "order one" wave superimposed on the mean density. However, some distortion (steepening or breaking) of that wave must occur before it can explain the field observations. The density profile for $\epsilon = 2$ is demonstrated in Fig. 5. Regions of the density profile are statically unstable. Such regions could overturn or flatten to form steps separated by high gradient sheets.⁽¹²⁾ This does, however, require waves of very large amplitude. We shall seek a mechanism that could transform waves of much smaller amplitude into fine structure. It will be shown that the most probable mechanism is the dynamic breaking of inertial waves.

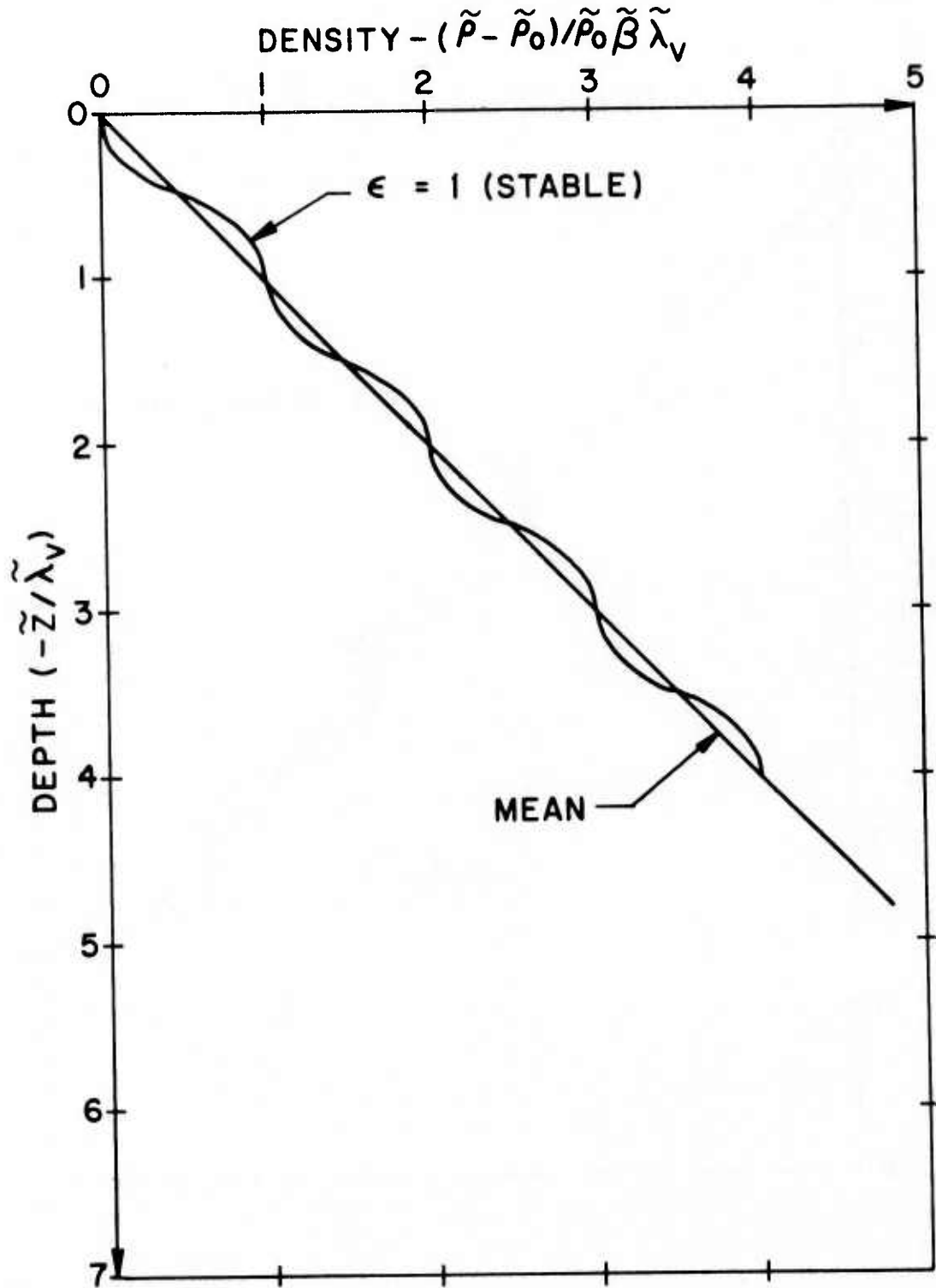


Fig. 4 Density Profile Corresponding to a Statically Stable Internal Wave

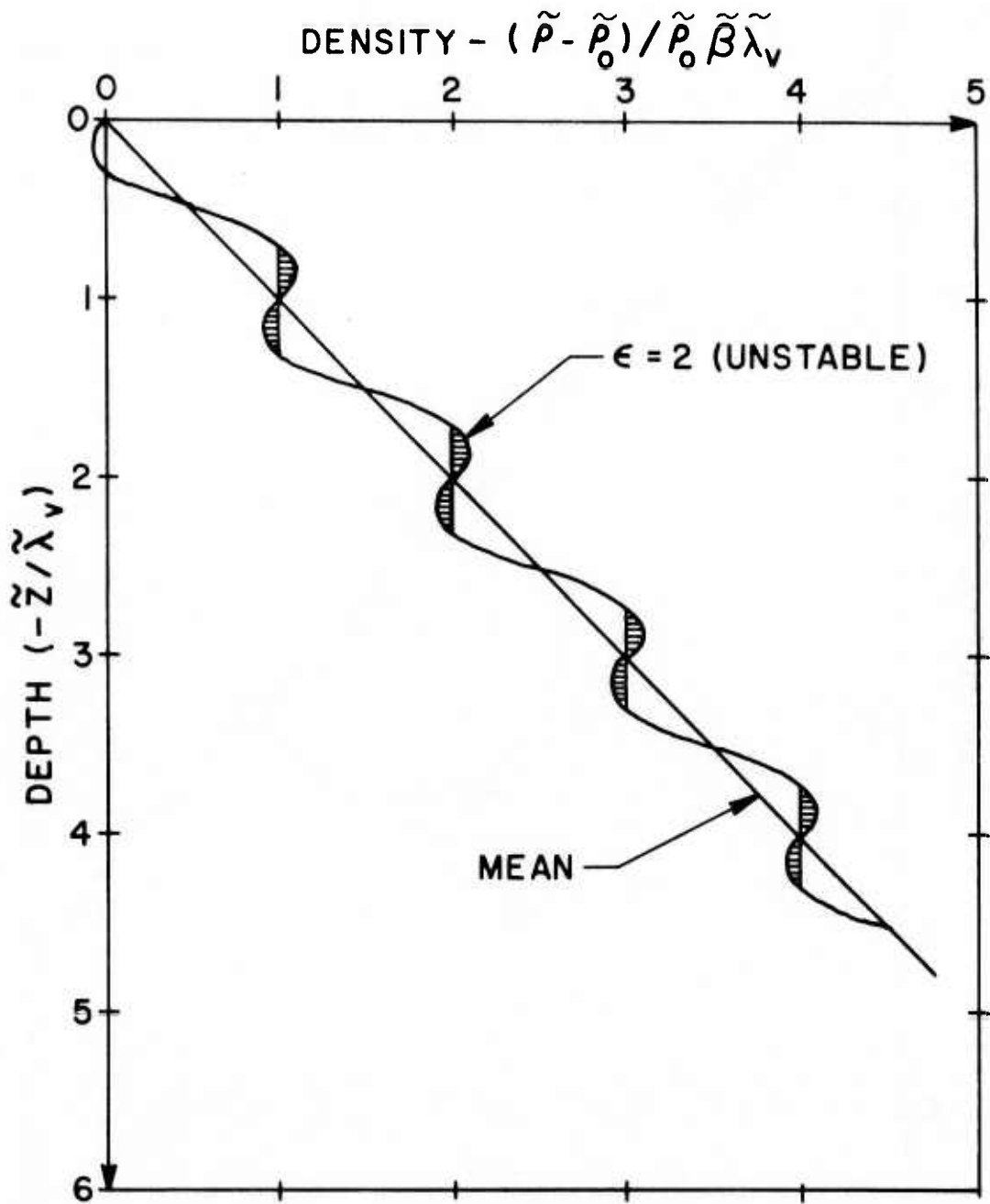


Fig. 5 Density Profile Corresponding to a Statically Unstable Internal Wave

III. COMPARISON OF FINE STRUCTURE DATA WITH INTERNAL WAVES

While we are not yet able to demonstrate that internal waves actually generate the ocean fine structure, we have several constraints on the waves which must be consistent with observation. Otherwise, they will never be capable of explaining the origin of the fine structure. We will now compare the fine structure length scales with those of internal waves, and then isolate the most probable mechanism responsible for generating the fine structure from the internal waves.

If internal waves cause fine structure, Figs. 4 and 5 suggest that $\tilde{\lambda}_v$ will correspond to the step \tilde{H} . Furthermore, we assert that $\tilde{\lambda}_H$, the horizontal wavelength, will correspond to the lateral extent of the fine structure. Therefore,

$$\delta_v \approx \frac{\text{Step Height}}{\text{Lateral Extent}}. \quad (15)$$

The field observations of δ_v are compared to the internal wave solutions in Fig. 6. While there is insufficient data to suggest a definite correlation, the data that is available does appear to correlate to inertial waves. This suggests that the mechanism responsible for generating fine structure may be inherent in the difference between inertial and gravity waves. That mechanism will be shown to be the dynamic stability of the wave.

There is a multitude of mechanisms that one could consider as a candidate for transforming inertial waves into fine structure. Basically, they can be classified into two major categories: stable and unstable. Internal waves may be driven unstable by a density inversion, more commonly referred to as a static instability, or by a dynamic instability. A primary example of a dynamic instability is the Kelvin-Helmholtz, or

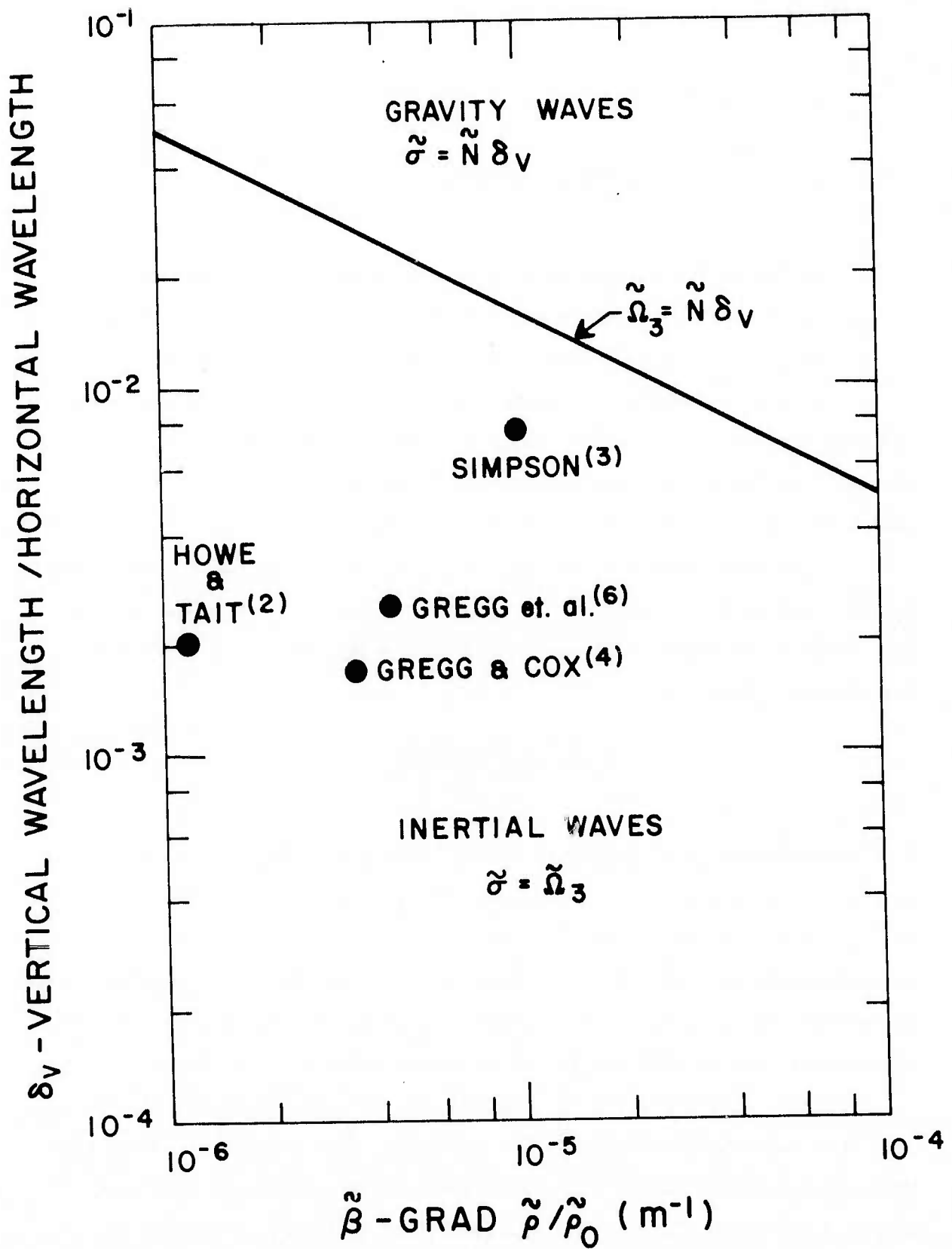


Fig. 6 Comparison of Internal Waves with Fine Structure

shear instability. Stable waves may be capable of generating fine structure through their nonlinear interaction with the velocity fields induced by the waves. This mechanism can be divided into two classes: transverse and self steepening. Transverse steepening simply refers to situations where resonance occurs: two or more plane waves interact through their transverse velocity fields. Self steepening refers to the influence of a higher order longitudinal velocity field. Such a velocity field would transport fluid in the direction of wave propagation and cause self attenuation of the wave. These four mechanisms may be summarized as follows:

- 1) The dynamic breaking of a single wave due to shear instabilities.
- 2) Breaking of a single wave by static instabilities.
- 3) Transverse steepening (resonance) by several non-parallel plane waves.
- 4) Self steepening of a single plane wave by a higher order longitudinal velocity.

In addition to the mechanisms listed above, one could consider the simultaneous effect of the sum of any two, three or four mechanisms. However, this may be considered over-ambitious at this point in the development of a fine structure model.

Let us now assess each of the four possible mechanisms:

The dynamic stability of the wave is measured by the Richardson number J ,¹⁵

$$J = \frac{-g}{\tilde{\rho}_0} \frac{\partial \tilde{\rho}}{\partial z} \bigg/ \left(\frac{\partial \tilde{u}}{\partial z} \right)^2 = \delta_v^2 (1 - \epsilon \cos z) / \epsilon^2 \varphi^2, \quad (16)$$

where

$$\varphi = \tilde{\sigma} / \tilde{N}.$$

For $J > 1$, a shear instability is always stabilized by the stratification whereas for $0 < J < 1$, the wave is unstable, provided that the Reynolds number is sufficiently large. A negative Richardson number corresponds to a statically unstable wave. This occurs when $\epsilon > 1$ and was illustrated in Fig. 5. Subsequently, the discussion of dynamic stability will be restricted to $\epsilon < 1$.

For gravity waves, $\varphi \equiv \delta_v$. If $\epsilon < 1$ it follows that $J > 1$ and the waves are dynamically stable. We will now show that inertial waves are dynamically unstable. This basic difference in dynamic stability will explain why fine structure apparently correlates only to inertial waves.

Inertial waves correspond to $\delta_v < \varphi$. Hence, the Richardson number is less than unity for $\epsilon < 1$. The critical value of the wave amplitude necessary to induce unstable wave motion is obtained from Eq. (16) for $J = 1$.

$$\epsilon_{\text{crit}} = \delta_v \tilde{N}/\tilde{\Omega}_3 \quad (17)$$

The critical values of the inertial wave amplitude are illustrated in Fig. 7. Wave amplitudes between 5×10^{-2} and 0.5 are required to explain available data. Hence, dynamic instabilities would occur at lower wave amplitudes than would static instabilities ($\epsilon \approx 1$). The mechanism would also explain why fine structure seems to accompany only inertial waves.

The Richardson criterion for wave instability has been satisfied. However, a Reynolds number constraint must also be satisfied before we can state that the inertial waves which correspond to fine structure are unstable. Since an inertial wave is a vertically propagating transverse wave, it creates a horizontal shear flow of velocity \tilde{u}_p and thickness $(\tilde{k}_v)^{-1}$. The stability of such a flow is measured by the flow Reynolds number Re_f , where

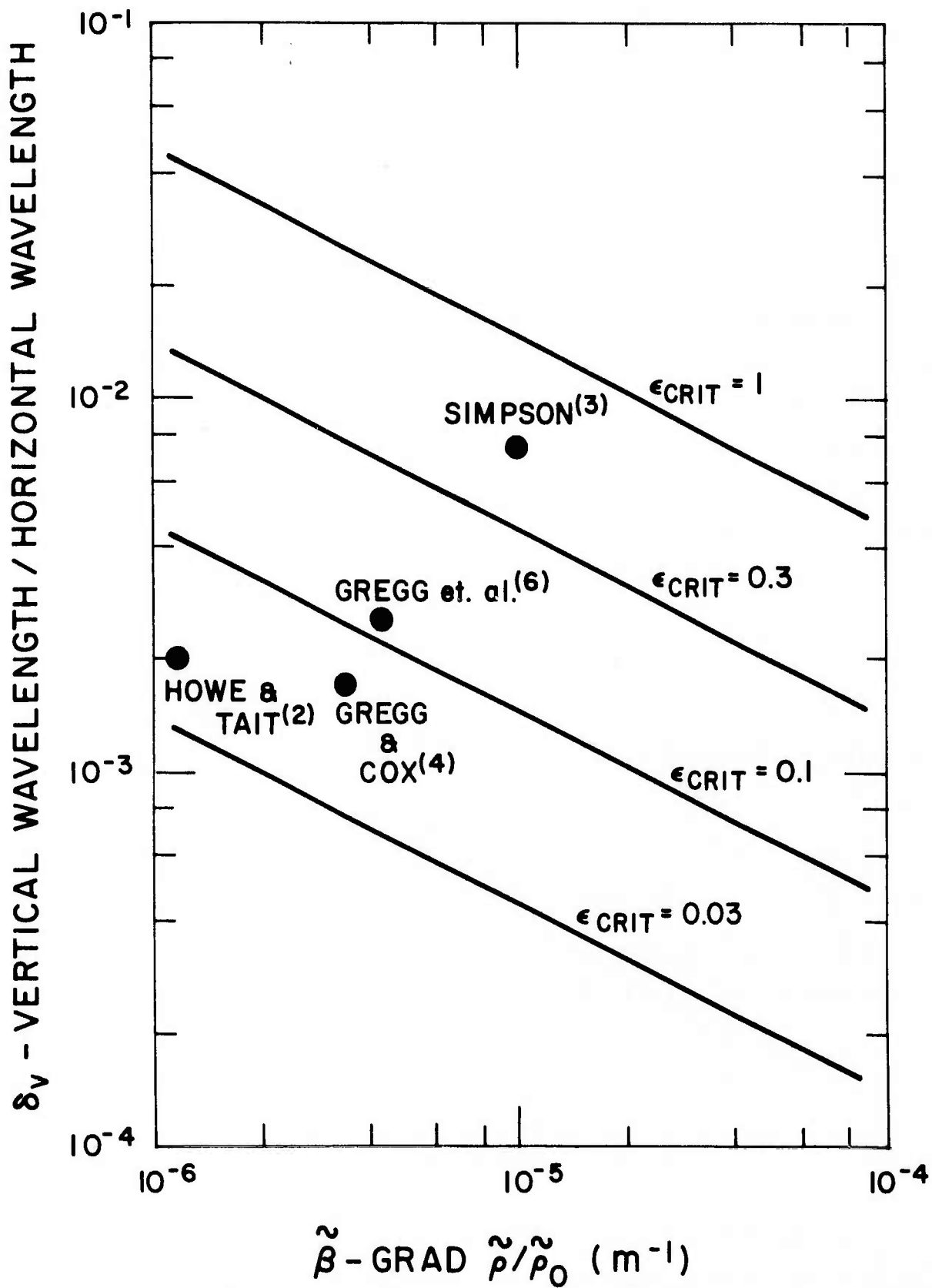


Fig. 7 Wave Amplitude Required for Instability

$$Re_f = \frac{\tilde{\rho}_o \tilde{u}_p}{\tilde{\mu} \tilde{k}_v} . \quad (18)$$

The transition value of Re_f is a function of the shape of the fluid velocity profile. For pipe flow and boundary layers, the transition Reynolds number is 2300 and 2700, respectively.¹⁶ Free shear layers have an inflection point in their velocity profile and are less stable than pipe and boundary layer flows. The transition Reynolds number for a free shear layer¹⁷ is of the order of 10 to 10^2 . Using the more restrictive value, we assert that the flow is unstable when

$$Re_f > 10^2 ,$$

or, using the definition of ϵ ,

$$\tilde{\lambda}_v \tilde{\lambda}_H > \frac{100 (2\pi)^2 \tilde{v}}{\epsilon \tilde{\sigma}} , \quad (19)$$

where $\tilde{v} = 2 \times 10^{-6} \text{ m}^2/\text{sec}$ and $\tilde{\sigma} = \tilde{\Omega}_3$. Instability will occur at a value of ϵ corresponding to ϵ_{crit} . Using ϵ_{crit} for ϵ , Eq. (19) becomes

$$\tilde{\lambda}_v > \frac{20\pi \sqrt{\tilde{v}}}{(\tilde{g}\tilde{\beta})^{1/4}} . \quad (20)$$

In addition to the constraint imposed by Eq. (20), the entire analysis requires that the mean motion be undamped. This was expressed as

$$\text{Re}_w > 1,$$

or

$$\tilde{\lambda}_v > \frac{2\pi \sqrt{\tilde{v}}}{\sqrt{\tilde{\Omega}_3}}. \quad (21)$$

The constraints imposed by Eqs. (20) and (21) are illustrated in Fig. 8. All fine structure data corresponds to dynamically unstable waves. This strongly indicates that shear instabilities are the mechanism by which inertial waves form fine structure. A mechanism utilizing shear instabilities was originally proposed by Woods and Wiley.¹¹ However, the present concept of unstable horizontal shear layers driven by vertically propagating inertial waves is quite different from Wood's concept of "Billow Turbulence" driven by gravity waves which propagate horizontally along density "sheets".

The second mechanism by which inertial waves may form fine structure is the static breaking of the wave due to a density inversion. This process was illustrated in Fig. 5. Large amplitude waves raise the heavier fluid to a position above the relatively lighter fluid. Static instabilities then break the wave and a staircase density profile results. While this is a reasonable postulate, it fails to explain why fine structure seems to correlate only to inertial waves. In addition, and most fundamental, the mechanism requires wave amplitudes an order of magnitude greater than those necessary to induce Kelvin Helmholtz instabilities. For this reason, static wave breaking will be considered a "low probability" candidate for the source of ocean fine structure.

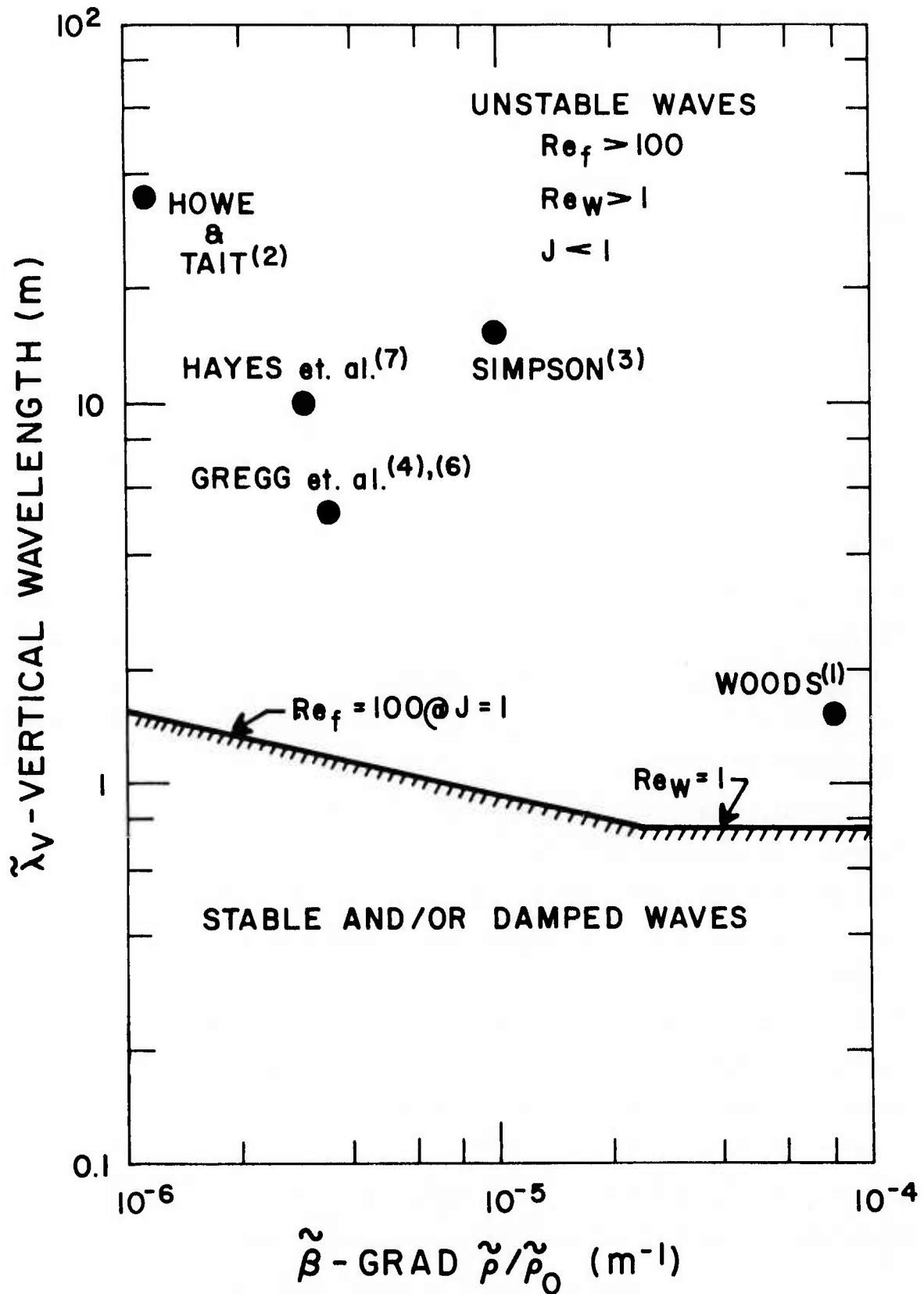


Fig. 8 Inertial Wave Stability

Transverse steepening or resonance was the third possible mechanism by which inertial waves could form fine structure. If the fine structure were created by the transverse resonance of perpendicular waves, then the persistence time of the fine structure would be of the order of $1/\tilde{\sigma}$ or, for inertial waves, a few hours. The fine structure data base (Table I) illustrates persistence times of the order of days. Thus, to explain fine structure with resonance, we would have to assume that both observers (Refs. 2 and 7) obtained their measurements an integral number of wave periods apart. Hayes et. al.⁽⁷⁾ obtained their data at 28°N. This corresponds to a wave period of 24 hrs. and would require three wave periods to be consistent with observation. Howe and Tait⁽²⁾ worked at 34°N, or 22 hr. wave periods. Hence, to explain "persistence times" of 33 hrs., we would have to invoke a resonance phenomenon occurring at the wave half period. While this is all possible, it does not seem highly probable. In order to explain fine structure on the basis of resonance we must invoke large wave amplitudes ($\epsilon \approx 1$). Inertial waves of that amplitude are dynamically unstable and incapable of undergoing a reversible energy exchange with other waves. Hence, resonance should also be considered to be a "low probability" candidate.

The fourth proposed mechanism is the self steepening of a plane wave due to a longitudinal velocity contained in the higher order terms of the dynamic equations. Such a mechanism requires that

$$\vec{U}_w \cdot \text{Grad } \vec{\xi} \neq 0,$$

where \vec{U}_w is the fluid velocity vector. For longitudinal, or acoustic sound waves, $\vec{U}_w \cdot \text{Grad } \vec{\xi}$ is an order ϵ term. Since inertial waves are, to

lowest order, transverse waves, self steepening can be no greater than an ϵ^2 effect. This is consistent with the self attenuation of surface waves. The dispersion equation⁽¹⁸⁾ yields a $(1 + \tilde{k}_H^2 \tilde{a}^2)$ term where \tilde{a} is the wave amplitude. Since $\tilde{a} \approx \tilde{u}_p / \tilde{\sigma}$, $\tilde{k}_H^2 \tilde{a}^2$ becomes ϵ^2 . Hence, self steepening requires ϵ^{-2} cycles to attenuate the wave. The maximum value of ϵ that we can use to estimate the steepening time in ϵ_{crit} because all waves corresponding to $\epsilon > \epsilon_{\text{crit}}$ are unstable. The steepening time $\tilde{\tau}_s$, becomes

$$\tilde{\tau}_s \doteq 2\pi / (\epsilon_{\text{crit}}^2 \tilde{\Omega}_3)$$

or

$$\tilde{\tau}_s \doteq \frac{2\pi \tilde{\Omega}_3}{\delta_v^2 \tilde{g} \tilde{\beta}}$$

Estimates of the self steepening times are illustrated in Fig. 9. Values of $\tilde{\tau}_s$ as large as 100 days are required in order to be consistent with data. It is difficult to believe than an inertial wave would not encounter several first order effects during this time period. These encounters would tend to destroy any coherence of the postulated mechanism. Hence, self steepening may also be considered "low probability".

Of the four mechanism proposed, dynamic wave breaking is the most probable mechanism by which inertial waves form fine structure. The wave length scales and the wave stability criterion are consistent with observation. However, it still remains to be demonstrated that a dynamically unstable inertial wave actually forms fine structure.

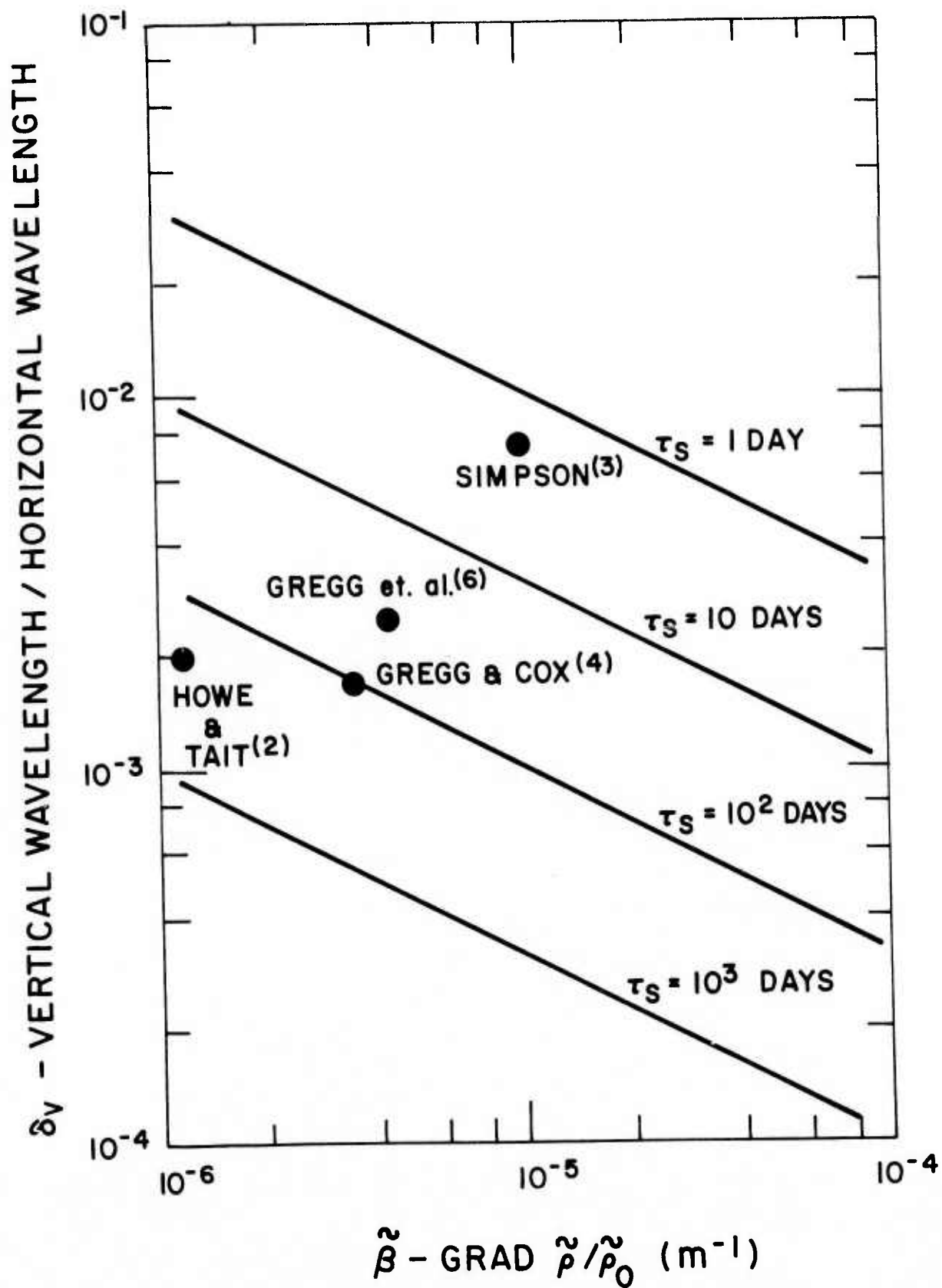


Fig. 9 Estimates of Self Steepening Times

IV. CONCLUSIONS

The preceding analysis has made an apparent correlation between ocean fine structure and inertial waves. A priori, there are four possible nonlinear mechanisms that could form ocean fine structure from inertial waves: dynamic breaking (shear instabilities), static breaking (inverted density profile), transverse steepening (resonance) and longitudinal steepening (self steepening of waves riding on their own velocity fields). Each mechanism has been assessed on the basis of the available data. Of the four mechanisms proposed, dynamic breaking is the most probable mechanism by which inertial waves form fine structure. The length scales of the wave and the stability criterion are consistent with observation. The static breaking of internal waves would require much larger wave amplitudes than does dynamic breaking. Hence, the concept of static instabilities becomes academic since these waves are already dynamically unstable. Resonance phenomenon would also require larger wave amplitudes than does the postulate of dynamic breaking. Thus, resonance cannot occur because inertial waves of the required amplitude are dynamically unstable. The possibility of self steepening has also been assessed. Estimates of the self steepening times for stable (low amplitude) inertial waves are of the order of 10^2 days. This is clearly a long time for an inertial wave to avoid other first order effects which could destroy the coherence of the mechanism. Hence, self steepening is a weak possibility compared to that of dynamic wave breaking.

Previous investigators¹¹ have proposed that shear instabilities lead to ocean fine structure. However, their concept was that of "Billow Turbulence" driven by gravity waves which propagate horizontally along density "sheets" (discontinuities in the vertical density profile). These gravity

waves break, mix and form the fine structure. The mechanism is illustrated in Fig. 10a. Figure 10b illustrates the present concept. A vertically propagating inertial wave generates a horizontal shear layer. The shear layer is dynamically unstable and appears to break, forming the fine structure. The wave length scales and stability criterion are consistent with fine structure observations. However, it still remains to be demonstrated that a dynamically unstable inertial wave actually forms fine structure.

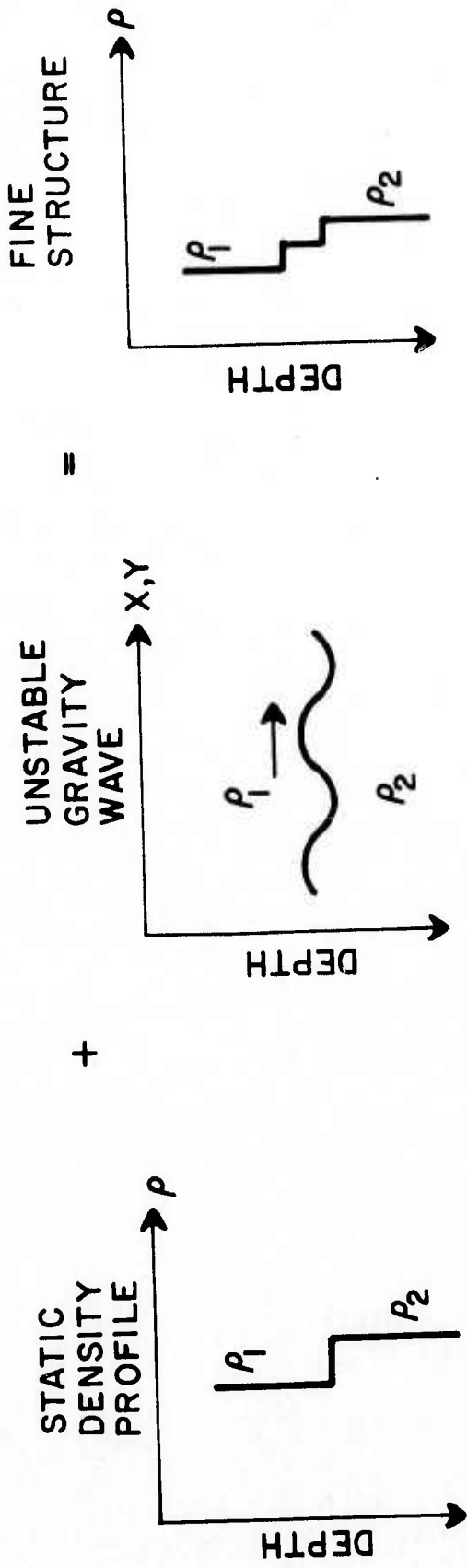


Fig. 10a Woods Postulate of Billow Turbulence

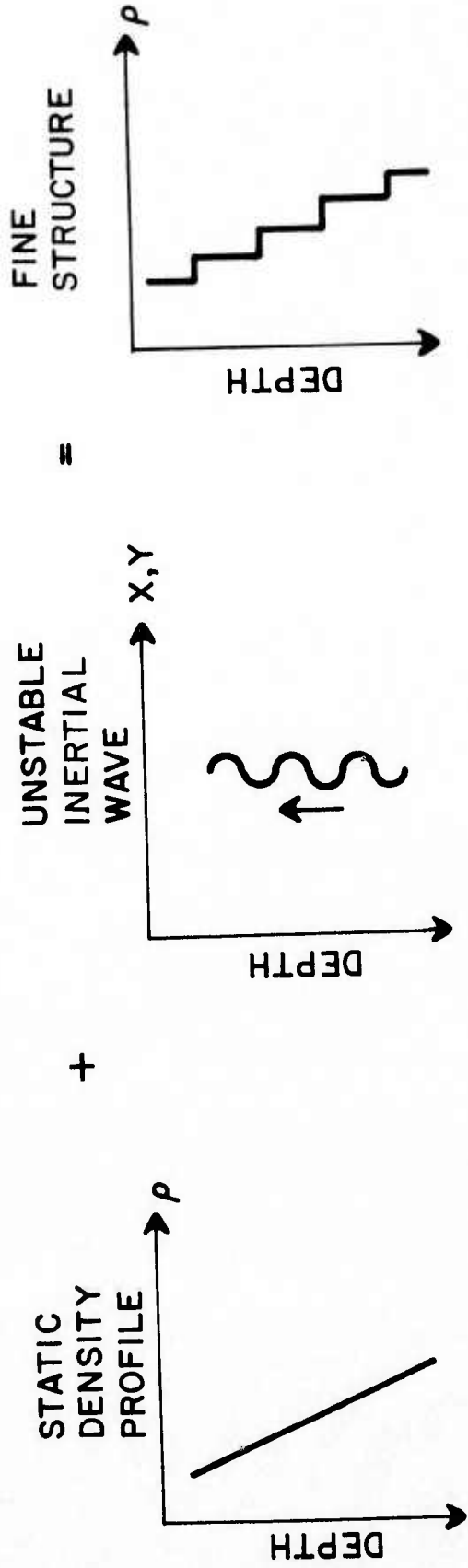


Fig. 10b Proposed Source of Ocean Fine Structure

REFERENCES

1. J. D. Woods, "Wave-Induced Shear Instability in the Summer Thermocline," *J. Fluid Mech.* (1968), Vol. 32, Part 4, pp. 791-800.
2. M. R. Howe and R. I. Tait, "Further Observations of Thermo-haline Stratification in the Deep Ocean," *Deep Sea Research*, 1970, Vol. 17, pp. 963-972.
3. J. H. Simpson, "Density Stratification and Microstructure in the Western Irish Sea," *Deep Sea Research*, 1971, Vol. 18, pp. 309 to 319.
4. M. C. Gregg and C. S. Cox, "The Vertical Microstructure of Temperature and Salinity," *Deep Sea Research*, 1972, Vol. 19, pp. 355 to 376.
5. T. R. Osborn and C. S. Cox, "Ocean Fine Structure," *Geophysical Fluid Dynamics*, 1972, Vol. 3, pp. 321 to 345.
6. M. C. Gregg, C. S. Cox and P. W. Hacker, "Vertical Microstructure Measurements in the Central North Pacific," *Journal of Physical Oceanography*, Vol. 3, No. 4, Oct. 1973, pp. 458 to 469.
7. S. P. Hayes, T. M. Joyce and R. C. Millard, Jr., "Measurements of Vertical Fine Structure in the Sargasso Sea," *Journal of Geophysical Research*, Vol. 80, No. 3, Jan. 1975, pp. 314 to 319.
8. M. C. Gregg, "Microstructure and Intrusions in the California Current," *Journal of Physical Oceanography*, Vol. 5, No. 2, April 1975, pp. 253 to 278.
9. M. E. Stern and J. S. Turner, "Salt Fingers and Convecting Layers," *J. Fluid Mech.* 16, pp. 497 to 511, 1969.
10. H. Stommel and K. N. Fedorov, "Small Scale Structure in Temperature and Salinity Near Timor and Mindanao," *Tellus*, 19, (2) pp. 307 to 325.
11. J. D. Woods and R. L. Wiley, "Billow Turbulence and Ocean Microstructure," *Deep-Sea Research*, 1972, Vol. 19, pp. 87 to 121.

12. I. Orlanski and K. Bryan, "Formation of the Thermocline Step Structure by Large-Amplitude Internal Gravity Waves", *J. Geophysical Research*, Vol. 74, No. 28, Dec. 20, 1969, pp. 6975 to 6983.
13. O. M. Phillips, The Dynamics of the Upper Ocean, Cambridge University Press, 1969, pp. 190-197.
14. O. M. Phillips, The Dynamics of the Upper Ocean, Cambridge University Press, 1969, p. 177.
15. O. M. Phillips, The Dynamics of the Upper Ocean, Cambridge University Press, 1969, p. 201.
16. H. Schlichting, Boundary Layer Theory, McGraw-Hill, 1955, pp. 309-310.
17. R. E. Esch, "The Instability of a Shear Layer Between Two Parallel Streams", *J. Fluid Mech.* Vol. 3, pp. 289-303 (1957).
18. O. M. Phillips, "Nonlinear Dispersive Waves", In Annual Review of Fluid Mechanics, Vol. 6, edited by M. Van Dyke Annual Reviews Inc., Palo Alto, California, 1974, p. 93.

ACKNOWLEDGEMENT

This research was supported by the Advanced Research Projects Agency of the Department of Defense and was monitored by ONR under Contract No. N00014-75-C-0927.

APPENDIX A
INTERNAL WAVE MODEL

Consider an orthogonal coordinate system on the surface of a rotating earth as shown in Fig. 3. The rotation vector is denoted by $\vec{\Omega}$ where \sim denotes a dimensional quantity. The coordinate system is chosen such that $\vec{\Omega}$ has no component in the \tilde{y} direction. Hence,

$$\vec{\Omega} = \tilde{\Omega}_1 \hat{i} + \tilde{\Omega}_3 \hat{k}, \quad (\text{A-1})$$

where

$$|\vec{\Omega}| = \frac{2\pi \text{ radians}}{12 \text{ hours}}.$$

The low Mach number motion associated with the ocean may be treated as incompressible. Hence, the Lagrangian derivative of density is zero.

$$\frac{D\tilde{\rho}}{D\tilde{t}} = 0 \quad (\text{A-2})$$

The equation of continuity then simplifies to

$$\vec{\nabla} \cdot \vec{U} = 0, \quad (\text{A-3})$$

where

$$\vec{U} = \tilde{u} \hat{i} + \tilde{v} \hat{j} + \tilde{w} \hat{k}. \quad (\text{A-4})$$

The momentum equation includes the influence of the Coriolis forces:

$$\frac{\partial \vec{U}}{\partial \tilde{t}} + \vec{\Omega} \times \vec{U} + (\vec{U} \cdot \vec{\nabla}) \vec{U} + \frac{1}{\tilde{\rho}} \vec{\nabla} p + g \hat{k} = \tilde{\nu} \nabla^2 \vec{U}, \quad (\text{A-5})$$

where $\tilde{\nu}$ is the kinematic viscosity and \tilde{g} is the acceleration of gravity.

Equations (A-2), (A-3) and (A-5) represent three equations in the density $\tilde{\rho}$, pressure \tilde{p} and the velocity \tilde{U} . To obtain a solution, we expand the dependent variables into a static and wave contribution:

$$\tilde{\rho} = \tilde{\rho}_0 + \tilde{\rho}_s(\tilde{z}) + \tilde{\rho}_w(\tilde{x}, \tilde{y}, \tilde{z}, \tilde{t}), \quad (\text{A-6})$$

$$\tilde{p} = \tilde{p}_0 - \tilde{\rho}_0 \tilde{g} \tilde{z} + \tilde{p}_s(\tilde{z}) + \tilde{p}_w(\tilde{x}, \tilde{y}, \tilde{z}, \tilde{t}), \quad (\text{A-7})$$

$$\tilde{u} = \tilde{u}_w(\tilde{x}, \tilde{y}, \tilde{z}, \tilde{t}), \quad (\text{A-8})$$

$$\tilde{v} = \tilde{v}_w(\tilde{x}, \tilde{y}, \tilde{z}, \tilde{t}), \quad (\text{A-9})$$

and
$$\tilde{w} = \tilde{w}_w(\tilde{x}, \tilde{y}, \tilde{z}, \tilde{t}), \quad (\text{A-10})$$

where we have restricted the analysis to zero mean shear. The only velocities are due to the wave contribution.

Setting all wave contributions equal to zero, we obtain the hydrostatic relationship between \tilde{p}_s and $\tilde{\rho}_s$,

$$\frac{\partial \tilde{p}_s}{\partial \tilde{z}} = - \tilde{\rho}_s(\tilde{z}) \tilde{g}.$$

The density profile in a static sea will be specified "a priori". Hence, we assert that

$$\frac{\partial \tilde{\rho}_s}{\partial \tilde{z}} = - \tilde{\beta} \tilde{\rho}_0,$$

where $\tilde{\rho}_0$ is the reference density at $\tilde{z} = 0$. The value of $\tilde{\beta}$ is expressed in units of inverse length and has values between $10^{-4}/\text{m}$ in the summer thermocline and $10^{-6}/\text{m}$ in the deep sea.

Substituting Eqs. (A-6) through (A-10) into (A-2), (A-3) and (A-5), we determine the equations of motion for the wave contribution:

$$\frac{\partial \tilde{\rho}_w}{\partial \tilde{t}} - \tilde{\rho}_0 \tilde{\beta}_w \tilde{w}_w + (\tilde{U}_w \cdot \tilde{\nabla}) \tilde{\rho}_w = 0, \quad (\text{A-11})$$

$$\tilde{\nabla} \cdot \tilde{U}_w = 0, \quad (\text{A-12})$$

and

$$\tilde{\rho} \left(\frac{\partial \tilde{U}_w}{\partial \tilde{t}} + \tilde{\Omega} \times \tilde{U}_w + \left(\tilde{U}_w \cdot \tilde{\nabla} \right) \tilde{U}_w \right) + \tilde{\nabla} \tilde{p}_w + \tilde{\rho}_w \tilde{g} \hat{k} = \tilde{\mu} \tilde{\nabla}^2 \tilde{U}_w, \quad (\text{A-13})$$

where $\tilde{\mu}$ is the viscosity.

We define the reference lengths as the inverse wave numbers in the horizontal and vertical directions:

$$\tilde{x}_{\text{ref}} = \tilde{y}_{\text{ref}} = \frac{\tilde{\lambda}_H}{2\pi} = \tilde{k}_H^{-1},$$

and

$$\tilde{z}_{\text{ref}} = \frac{\tilde{\lambda}_V}{2\pi} = \tilde{k}_V^{-1}.$$

The horizontal fluid velocity is normalized to \tilde{u}_p , an arbitrary velocity which will be related to the wave amplitude.

$$\tilde{u}_{\text{ref}} = \tilde{v}_{\text{ref}} = \tilde{u}_p$$

The continuity equation suggests that the reference velocity in the \tilde{z} direction is

$$\tilde{w}_{\text{ref}} = \tilde{u}_p \tilde{k}_H / \tilde{k}_V.$$

The reference time is the inverse frequency, which will be determined from the wave equations.

$$t_{\text{ref}} = 1/\tilde{\sigma}$$

The linear form of Eq. (A-11) suggests the reference density,

$$\tilde{\rho}_{\text{ref}} = \tilde{u}_p \tilde{\rho}_o \tilde{\beta} \tilde{k}_H / \tilde{\sigma} \tilde{k}_v.$$

In the vertical momentum equation, it is not clear whether the vertical pressure gradient should balance the buoyancy, or the Coriolis force. Hence, we normalize the pressure by the buoyant terms

$$\tilde{p}_{\text{ref}} = Q \tilde{\rho}_o \tilde{u}_p \tilde{\sigma} / \tilde{k}_H,$$

but introduce the ordering parameter Q which must be determined.

The reference variables are used to define the following dimensionless parameters:

$$\epsilon = \tilde{u}_p \tilde{k}_H / \tilde{\sigma} \quad (\text{Wave Amplitude}),$$

$$\Delta = \tilde{\beta} / \tilde{k}_v \quad (\text{Static } \Delta\rho/\rho \text{ Across Wave}),$$

$$\delta_v = \tilde{k}_H / \tilde{k}_v \quad (\text{Vertical/Horizontal Length Scale}),$$

and

$$\text{Re}_w = \tilde{\rho}_o \tilde{\sigma} / \tilde{\mu} \tilde{k}_v^2 \quad (\text{Wave Reynolds Number}).$$

The frequencies $\tilde{\sigma}$ and $\tilde{\Omega}$ are normalized to \tilde{N} , the Brunt Väisälä frequency, which is assumed to be constant.

$$\tilde{N}^2 = \tilde{g} \tilde{\beta}$$

$$\varphi = \tilde{\sigma} / \tilde{N}$$

$$\vec{\omega} = \tilde{\Omega} / \tilde{N}$$

The equations of motion for the wave contribution are non-dimensionalized. The statement of incompressibility becomes

$$\frac{\partial \rho_w}{\partial t} - w_w + \epsilon (\vec{U}_w \cdot \vec{\nabla} \rho_w) = 0, \quad (\text{A-14})$$

where

$$\vec{\nabla} = \delta_v \frac{\partial}{\partial x} \hat{i} + \delta_v \frac{\partial}{\partial y} \hat{j} + \frac{\partial}{\partial z} \hat{k}$$

and

$$\vec{U}_w = \frac{u_w}{\delta_v} \hat{i} + \frac{v_w}{\delta_v} \hat{j} + w_w \hat{k}$$

such that

$$\vec{U}_w \cdot \vec{\nabla} = O(1).$$

The equation of continuity is expressed as

$$\vec{\nabla} \cdot \vec{U}_w = 0, \quad (\text{A-15})$$

and, expanding $\tilde{\rho}$,

$$\frac{\tilde{\rho}}{\rho_0} = \Lambda = 1 - \Delta z + \Delta \epsilon \rho_w,$$

the x, y, and z momentum equations become, respectively,

$$\Lambda \left[\varphi \frac{\partial u_w}{\partial t} + \epsilon \varphi (\vec{U}_w \cdot \vec{\nabla}) u_w - \omega_3 v_w \right] + \varphi Q \frac{\partial p_w}{\partial x} = \left(\frac{\varphi}{\text{Re}_w} \right) \nabla^2 u_w, \quad (\text{A-16})$$

$$\Lambda \left[\varphi \frac{\partial v_w}{\partial t} + \epsilon \varphi (\vec{U}_w \cdot \vec{\nabla}) v_w + \omega_3 u_w - \delta_v \omega_1 w_w \right] + \varphi Q \frac{\partial p_w}{\partial y} = \left(\frac{\varphi}{\text{Re}_w} \right) \nabla^2 v_w, \quad (\text{A-17})$$

and

$$\Lambda \left[\varphi^2 \delta_v^2 \frac{\partial w_w}{\partial t} + \epsilon \delta_v^2 \varphi^2 (\vec{U}_w \cdot \vec{\nabla}) w_w + \omega_1 \delta_v \varphi v_w \right] + Q \varphi^2 \frac{\partial p_w}{\partial z} + \delta_v^2 \rho_w = \delta_v^2 \left(\frac{\varphi^2}{\text{Re}_w} \right) \nabla^2 w_w. \quad (\text{A-18})$$

Linear Solution

In the limit of $\epsilon \ll 1$, $\Delta \ll 1$ and $\text{Re}_w \gg 1$, Eqs. (A-14) through (A-18) are a linear system. From Phillips⁽¹³⁾ we know that w_w possesses a wave solution where the frequency is given by

$$\tilde{\sigma}^2 = \tilde{N}^2 \delta_v^2 / (1 + \delta_v^2) + (\vec{\Omega} \cdot \hat{\mu})^2, \quad (\text{A-19})$$

where $\hat{\mu}$ is a unit vector in the direction of the wave propagation,

$$\hat{\mu} = \delta_1 \delta_v \hat{i} + \delta_2 \delta_v \hat{j} + \hat{k},$$

where

$$\delta_1 = \tilde{k}_x / \tilde{k}_H,$$

$$\delta_2 = \tilde{k}_y / \tilde{k}_H,$$

and

$$\delta_1^2 + \delta_2^2 = 1.$$

The linear wave solution for w_w is

$$w_w = A \exp(i \xi),$$

where A is an arbitrary constant and ξ is given by

$$\xi = t + \delta_1 x + \delta_2 y + z.$$

From Eq. (A-14), the density is obtained from the vertical velocity,

$$\rho_w = -i A \exp(i \xi).$$

In the limit of $\delta_v < 1$, Eq. (A-19) yields the nondimensional frequency,

$$\varphi^2 = \delta_v^2 + (\vec{\omega} \cdot \hat{\mu})^2. \quad (\text{A-20})$$

Eq. (A-20) indicates that there are two limits in which the momentum equations must be solved for u_w , v_w , and p_w . Those limits depend on the relative size of δ_v and $(\vec{\omega} \cdot \hat{\mu})$, the buoyant and inertial frequencies respectively.

For Gravity Waves ($\delta_v > (\vec{\omega} \cdot \hat{\mu})$), the solutions become

$$\varphi = \delta_v,$$

$$Q \equiv 1,$$

$$p_w = A \exp(i \xi),$$

$$u_w = -\delta_1 A \exp(i \xi),$$

and

$$v_w = -\delta_2 A \exp(i \xi).$$

For Inertial Waves ($(\vec{\omega} \cdot \hat{\mu}) > \delta_v$), the solutions are

$$Q \ll 1,$$

$$\varphi \equiv \omega_3,$$

$$u_w = i(\delta_2 + i\delta_1) A \exp(i \xi),$$

and

$$v_w = -(\delta_2 + i\delta_1) A \exp(i \xi).$$

The inertial solution of the vertical momentum equation yields different results for p_w depending upon the relative size of δ_v and φ^2 .

Physically, the different solutions arise due to the relative size of the buoyant and Coriolis forces.

For Inertial Gravity Waves (buoyancy balances pressure), we obtain

$$\varphi^2 < \delta_v < \varphi,$$

$$Q = \delta_v^2 / \varphi^2,$$

and

$$p_w = A \exp(i \xi).$$

For Pure Inertial Waves (Coriolis force balances pressure), we obtain

$$\delta_v < \varphi^2,$$

$$Q = \delta_v,$$

and

$$p_w = -i \left(\frac{\omega_1}{\omega_3} \right) (\delta_2 + i \delta_1) A \exp(i\xi).$$

The regimes of $(\tilde{\beta}, \delta_v)$ space appropriate to gravity waves, inertial gravity waves and pure inertial waves are illustrated in Fig. (A-1). The solutions appropriate to each regime were given above.

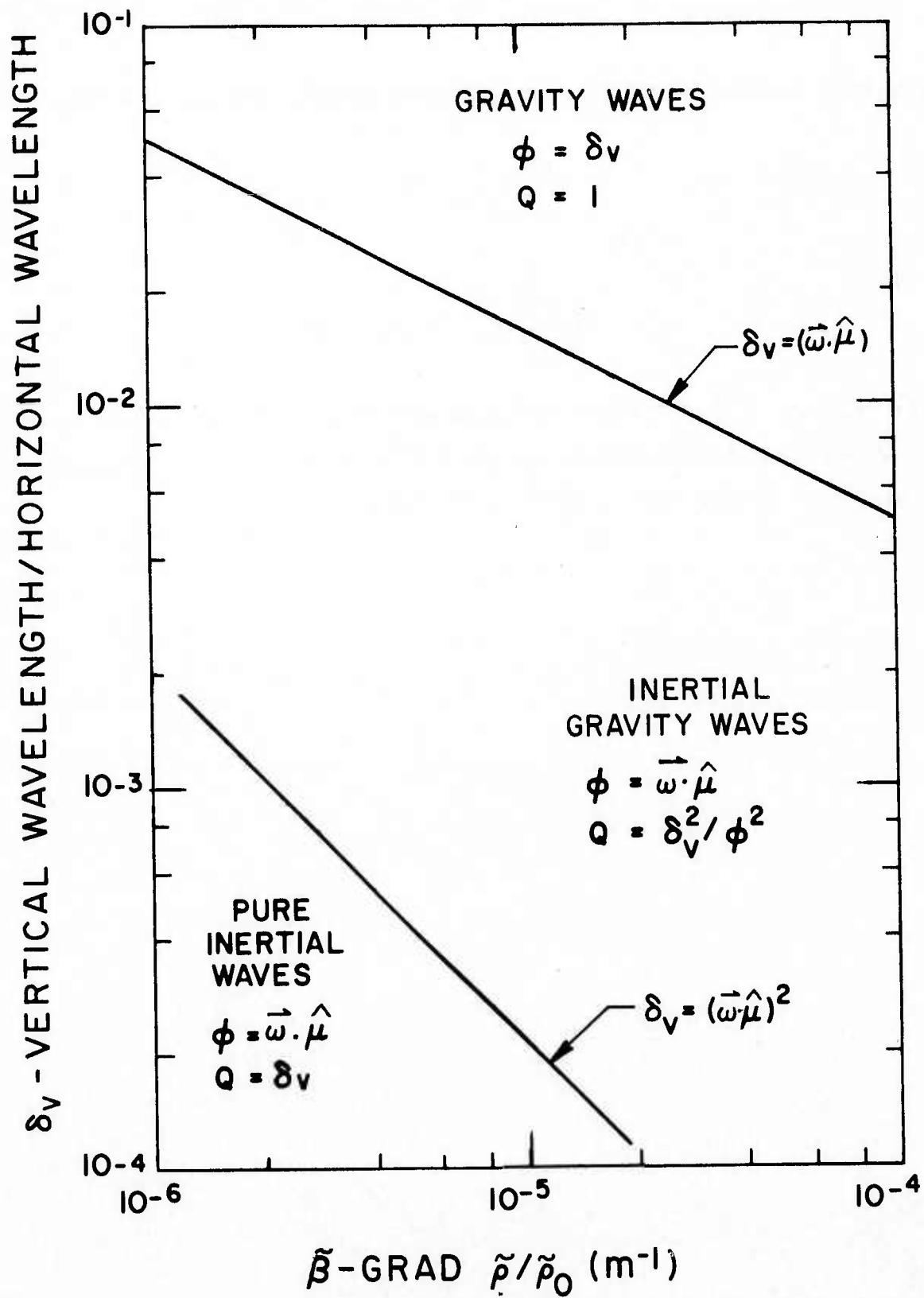


Fig. A-1 Internal Wave Regimes